Activation of G protein-coupled receptors : the role of extracellular loops in adenosine receptors

Peeters, M.C.

CHAPTER 3

GPCR STRUCTURE AND ACTIVATION: AN ESSENTIAL ROLE FOR THE FIRST EXTRACELLULAR LOOP IN ACTIVATING THE ADENOSINE A_{2B} RECEPTOR

This chapter was based upon:

M.C. Peeters, D. Guo, G.J.P van Westen, L.E. Wisse, M.W. Beukers, A.P. IJzerman. FASEB journal **2011**, 25(2):632-43

ABSTRACT

The highly variable extracellular loops in G protein-coupled receptors (GPCRs) have been implicated in receptor activation, the mechanism of which is poorly understood. In a random mutagenesis screen on the human adenosine A_{2B} receptor ($A_{2B}R$) using the MMY24 *Saccharomyces cerevisiae* strain as a read-out system, we found that two residues in the first extracellular loop, a phenylalanine and an aspartic acid at positions 71 and 74, respectively, are involved in receptor activation. We subsequently performed further site-directed and site-saturation mutagenesis. These experiments revealed that the introduction of mutations at either of the identified positions results in a wide variety of receptor activation profiles, with changes in agonist potency, constitutive activity, and intrinsic activity. Radioligand binding studies showed that the changes in activation were not due to changes in receptor expression. We interpret these data in the light of the recently revealed structure of the adenosine $A_{2A}R$, the closest homologue of the $A_{2B}R$. The two residues are suggested to be vital in maintaining the tertiary structure of a β-sheet in the extracellular domain of the $A_{2B}R$. We hypothesize that deterioration of structure in the extracellular domains of GPCRs compromises overall receptor structure with profound consequences for receptor activation and constitutive activity.

INTRODUCTION

Recently, considerable progress has been made in understanding the structure of G protein-coupled receptors (GPCRs) and their mechanisms of activation. The highly variable extracellular region of GPCRs is increasingly recognized as an important determinant in receptor activation, next to the intracellular and transmembrane domains [1,2,3,4,5]. However, for many GPCRs it is still poorly understood how the N-terminus and extracellular loops are able to influence receptor activation. The extracellular domains have been reported as managers of activation, either by keeping the receptor in a silent state or by stabilizing the active conformation of the receptor [3,6,7]. Several recent reports have shown that all extracellular regions together, including the hinge region, are required for full TSH receptor activation with the first extracellular loop (EL1) as a key player [8,9,10].

In this study, we have investigated the first extracellular loop in the adenosine A_{2B} receptor (A_{2B}R), a typical class A GPCR. Four subtypes of adenosine receptors are known (A_1R, A_{2A}R, A_{2B}R, and A_3R), all of which are ubiquitously expressed in the human body [11]. Although all four subtypes respond to the same endogenous ligand adenosine, they target different intracellular signaling pathways. The A_1R and the A_3R subtypes mainly signal through G_i proteins mediating the inhibition of adenylyl cyclase, which leads to decreased levels of cAMP in the cell. The A_{2A}R and A_{2B}R cause an increase in intracellular cAMP levels by coupling mainly to G_s proteins resulting in the activation of adenylyl cyclase [12]. Of the adenosine subfamily, the A_{2B}R subtype has been investigated least. However, the adenosine A_{2B} receptor is an interesting drug target as it has been implicated in asthma [13], chronic obstructive pulmonary disease (COPD) [14], and other inflammatory diseases [15].

Here, we report a useful and fast approach to elucidate receptor activation mechanisms using successive mutagenesis experiments. We started with an unbiased random mutagenesis screen for increased activity in a robust yeast system. The *S. cerevisiae* strain used to evaluate receptor activation has been genetically modified to serve as a reporter system with growth as an output parameter. This yeast system is an ideal background to monitor activation of a single GPCR, since its only endogenous GPCR has been removed from the system while still maintaining the complete GPCR signaling machinery [16]. Several previous reports have proved this eukaryotic system to be predictive of the mammalian situation [17,18].

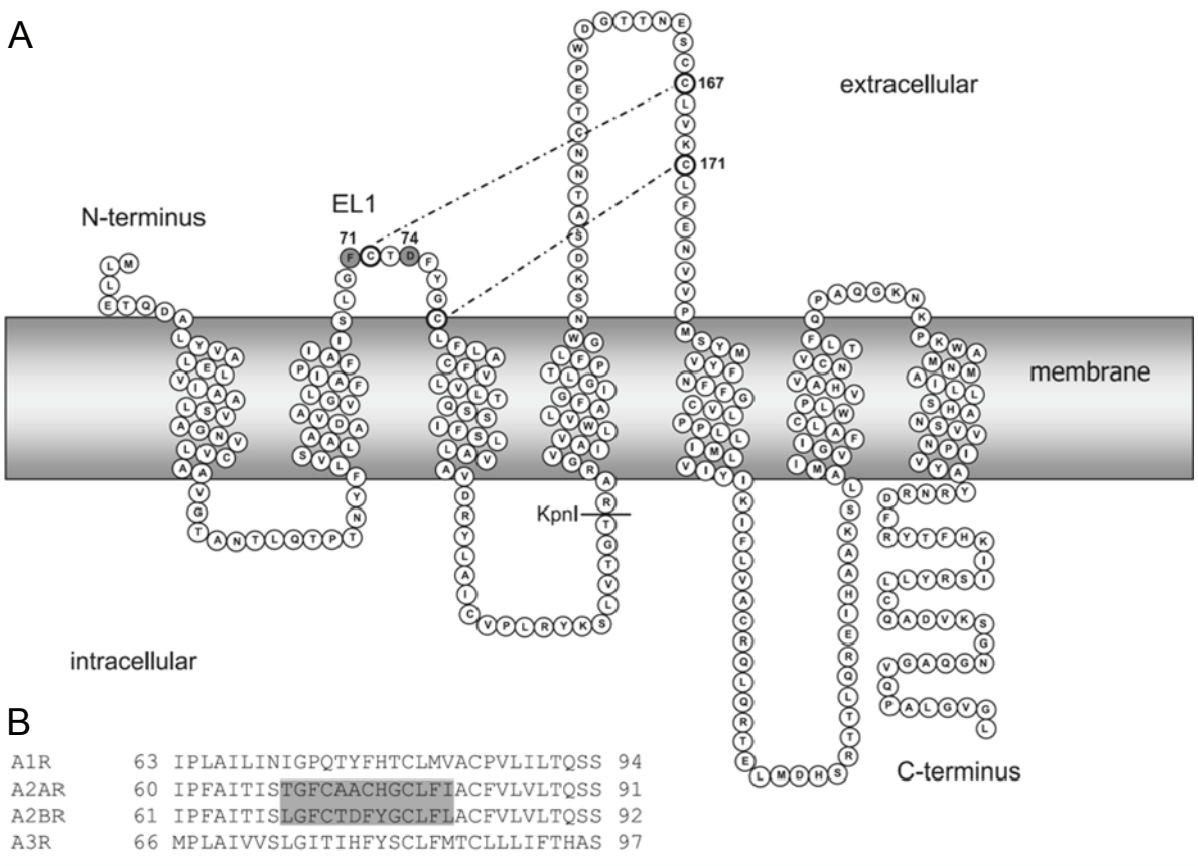

Figure 1. (*A*) Snake plot of the adenosine A_{2B}R. Residues F71 and D74 in the first extracellular loop of the A_{2B}R are shaded. Dotted lines indicate disulfide bridges. The disulfide bridge conserved in many class A GPCRs links C78 and C171. The nonconserved second disulfide bridge between EL1 and EL2, based on the crystal structure of the adenosine A_{2A}R (PDB: 3EML), links C72 and C167. In the second intracellular loop, the restriction site *Kpn*I that was used to obtain the fragment for random mutagenesis is indicated. (*B*) Multiple sequence alignment of the 4 adenosine receptor subtypes. Shading indicates the sequence of EL1 that was substituted in the creation of the chimeric A_{2A}R-A_{2B}R model in Figure 8.

From a random mutagenesis screen Beukers et al. [18] previously identified mutations located in the transmembrane domains and the intracellular regions of the A_{2B}R that caused high receptor constitutive activity. In the present study we investigated a mutant receptor with two mutated residues in the first extracellular loop, consisting of a phenylalanine and an aspartic acid that are involved in receptor activation (**Figure 1**). These residues were not predicted to be important for adenosine receptor activation by any rational approach. The two positions were further characterized by site-directed mutagenesis and subsequent site-saturation mutagenesis, further emphasizing the involvement of positions 71 and 74 in receptor structure and activation. The importance of maintaining receptor structure was corroborated by the recently published structure of the adenosine A_{2A}R, the closest homologue of the A_{2B}R [4]. To our knowledge, this is the first report that describes

the large influence of structural features at the extracellular region on receptor activation. It is likely that similar features are involved in the activation mechanism of other GPCRs, even though the specific three-dimensional structures will most likely differ between subfamilies or even subtypes.

MATERIALS AND METHODS

Random Mutagenesis

A KpnI restriction site was introduced in the adenosine A_{2B} receptor gene in the region encoding the second intracellular loop, making it possible to obtain a fragment with a suitable size for random mutagenesis [19]. Random mutations were induced in the fragment consisting of the first 372 base pairs of the A_{2B}R gene by using an error prone PCR method adapted from Fromant et al. [20]. The mutagenized fragments were subsequently reintroduced in an otherwise wild type A_{2B} receptor. The random mutagenized A_{2B}R library was obtained as described earlier by Beukers et al. [18].

Site-directed Mutagenesis

Site-directed mutants A_{2B}R_F71L and A_{2B}R_D74G were constructed by PCR mutagenesis using pDT-PGK_$A_{2B}R_{KpnI}$ as a template. The mutant A_{2B}R_F71L was created using primers containing an EcoR31I site for directional PCR product cloning purposes. The EcoR31I restriction enzyme was purchased from Fermentas (St. Leon-Rot, Germany). The primers used for the site-directed mutagenesis were:

5'-CATCATGGTCTCAGAAGTCAGTGCAGAGGCCCAGGC-3'

5'-CATCATGGTCTCACTTCTACGGCTGCCTCTTCC-3'

The mutant A_{2B}R_D74G was generated by Baseclear (Leiden, The Netherlands). For this purpose, the following primers were used:

5'-CAGCCTGGGCTTCTGCACTGGCTTCTACGGCTGCCTCTTCC-3'

5-'GGAAGAGGCAGCCGTAGAAGCCAGTGCAGAAGCCCAGGCTG-3'

Both mutant receptor genes were verified by double-stranded sequencing (LGTC, Leiden, The Netherlands).

Site-saturation Mutagenesis

Site-saturation mutagenesis on positions 71 and 74 in the first extracellular loop of the human adenosine A_{2B} receptor was performed based on the QuickChange Multi-Site Directed Mutagenesis system (Stratagene, Huizen, The Netherlands). The plasmid pDT-PGK_$A_{2B}R_{KpnI}$ was used as the template in this PCR-based mutagenesis method. The following primers containing a randomized codon at the sites of interest were used:

F71N: T211N_T212N_C213N 5'ATCACCATCAGCCTGGGCNNNTGCACTGACTTCTACGGC-3'

D74N: G220N_A221N_C222N 5'AGCCTGGGCTTCTGCACTNNNTTCTACGGCTGCCTCTTC-3'

Prior to transformation of the single stranded plasmids into XL10 Gold Chemical Competent *E.Coli* cells, the PCR product was treated with DpnI to remove methylated template. After selection on LB-Amp agar plates, 100 isolated plasmids from each mutagenesis project were chosen for identification by DNA sequencing to retrieve as many amino acid changes at the positions as possible.

Transformation in MMY24 S. cerevisiae strain

pDT-PGK_$A_{2B}R$ plasmids were transformed into an *S. cerevisiae* yeast strain according to the Lithium-Acetate procedure. The strain is derived from the MMY11 strain [21] and was further adapted to communicate with mammalian GPCRs through the introduction of a chimeric G protein [16]. The genotype of the MMY24 strain is: *MAT**a**his3 leu2 trp1 ura3can1 gpa1_::G_i3 far1_::ura3 sst2_::ura3 Fus1::FUS1-HIS3 LEU2::FUS1-lacZ ste2_::G418R.* To measure signaling of GPCRs, the pheromone signaling pathway of this strain was coupled via the FUS1 promotor to HIS3, a gene encoding the key enzyme in histidine production, imidazole glycerol-phosphate dehydrase. The degree of receptor activation was measured by the growth rate of the yeast on histidine-deficient medium.

Screening for increased activation in S. cerevisiae

The mutant $A_{2B}R$ library was screened in a yeast system for constitutively active receptors and/or receptors showing an increased potency of the full $A_{2B}R$ agonist 5'-N-ethylcarboxamidoadenosine (NECA) (Sigma-Alderich, Zwijndrecht, The Netherlands).The random mutagenesis screen was performed as described earlier by Beukers et al. [18]. The plasmid containing the $A_{2B}R$_F71L/D74G mutant identified from this screen was isolated and retransformed into the MMY24 yeast strain.

Solid growth assay

To characterize the mutant receptors further, concentration-growth curves were generated in a solid growth assay. In this assay, yeast cells from an overnight culture were diluted to around 400,000 cells/ml (OD_{600} ≈ 0.02), and droplets of 1.5 µl were spotted on selection agar plates, YNB-ULH, containing 7 mM 1,2,4-aminotriazole (3-AT) (Sigma-Alderich, Zwijndrecht, The Netherlands) and a NECA concentration ranging from 10^{-9} to 10^{-5} M. When monitoring responsiveness to an inverse agonist, ZM241385 (final concentration 10^{-5}M) was added to the selection plates [22]. A concentration range from 10^{-9} to 10^{-5} M was used in the concentration-growth curves with BAY 60-6583 (synthesized in house), a non-nucleoside agonist [23]. After incubation at 30°C for 50 h, the plates were scanned and receptor-mediated yeast growth was quantified with Quantity One imaging software from Bio-Rad (Hercules, CA). The amount of growth of yeast was calculated as the density of each spot with a correction for local background on the plate. Data were analyzed using nonlinear regression analysis software available in GraphPad Prism 5.0 (GraphPad Software, San Diego, CA).

Schild plot analysis

For the wild type A_{2B} receptor and for the mutant receptor D74W, concentration-growth curves of agonist NECA were recorded in the presence of increasing concentrations of the selective A_{2B}R antagonist PSB603. Schild analysis was performed using the appropriate equations available in GraphPad Prism 5.0.

Whole cell extracts and immunoblotting

Whole protein cell extracts were made from the transformed yeast cells using trichloroacetic acid (TCA). From an overnight culture, $1.2 \cdot 10^8$ yeast cells were harvested in mid-log phase. The cells were washed twice with 20% TCA after which they were broken by vigorous vortexing in the presence of glass beads. The yeast cell extracts were separated using SDS/PAGE and subsequently blotted on Hybond-ECL membranes. For this purpose, a sample of 4.0 µl containing 12 µg protein was loaded on a 12.5% SDS/PAGE gel. A semi-automated electrophoresis technique (PhastSystem™, Amersham Pharmacia Biotech) was used for SDS/PAGE as well as blotting. The antibody directed against the C-terminal region of the adenosine A_{2B} receptor was kindly provided by by Dr. I. Feoktistov (Vanderbilt University, Nashville).

Densitometric analysis of the protein bands was performed using the volume analysis tool present in the Quantity One imaging software from Bio-Rad (Hercules, CA). The aspecific band at approximately 45 kDa was used as loading control. The ratio between specific $A_{2B}R$ protein bands and aspecific bands was determined and the wild type receptor was set at 100%, the empty vector pDT-PGK at 0%. The experiment was performed in duplicate.

Whole cell radioligand binding experiments

Yeast cells expressing wild type or mutated $A_{2B}R$ were cultured overnight in rich YAPD medium. Cells were centrifuged for 5 minutes at 2000 x *g*, the pelleted cells were once washed with 0.9% NaCl. The cells were again centrifuged 5 minutes at 2000 x *g* and diluted in the assay buffer (50 mM Tris-HCl pH7.4 + 1 mM EDTA) to OD_{600}=40 (OD_{600} = 1 ≈ $2.5 \cdot 10^7$ cells/ml). Binding experiments were performed with 0.5-0.8 nM [^{3}H]PSB-603 and a final cell concentration of $25 \cdot 10^7$ cells/ml in a total volume of 100 µl [24]. Nonspecific binding was determined in the presence of 1 mM NECA. Samples were incubated for 1 hour at 25ºC while shaking vigorously to keep the yeast cells in suspension. Incubation was terminated by adding 1 ml ice-cold assay buffer. Bound from free radioligand was immediately separated by rapid filtration through Whatman GF/B filters pre-incubated with 0.1% polyethylenimine (PEI) using a Millipore manifold during which the filters were washed six times with ice-cold assay buffer. Filter-bound radioactivity was determined by scintillation spectrometry (Tri-Carb 2900TR; PerkinElmer Life and Analytical Sciences) after addition of 3.5 ml of PerkinElmer Emulsifier Safe.

Receptor homology modeling

The adenosine A_{2A} receptor is the closest homologue of the adenosine A_{2B} receptor, with 82.1 % amino acid similarity and 59.4 % identity. Recently, the high resolution crystal structure of the human adenosine A_{2A} receptor was published (PDB entry code: 3EML) [4]. A chimeric $A_{2B}R$-$A_{2A}R$ model was created in the Molecular Operating Environment (MOE) software package, version 2008.10 [25]. In this model, only the first extracellular loop of $A_{2A}R$ (T68–I80) was replaced by the residues making up the first extracellular loop of the $A_{2B}R$ (L69-L81) (**Figure 1B**). Since the remaining parts of the chimeric receptor were kept as they are in the $A_{2A}R$, this constitutes a partial homology model. Subsequently, a limited molecular mechanics

optimization was performed to reposition the residue side chains present in the EL1 and the neighboring EL2 in an optimal energetic state after substitution. The side chains were therefore able to form aromatic, charged and cysteine-cysteine interactions after the substitution, confirming the validity of the substitution. The optimization was performed using the AMBER99 force field, parameterized particularly for proteins and nucleic acids, as implemented in MOE [26]. The end result was a model of the A_{2A}R that carried the first extracellular loop of the A_{2B}R.

RESULTS

Random Mutagenesis

For the purpose of random mutagenesis, a limited sized fragment of 372 base pairs was used starting from the ATG until the KpnI site in the second intracellular loop. The KpnI restriction site was introduced by site-directed mutagenesis, resulting in a silent mutation. The fragment of interest encodes for the N-terminus, the first three transmembrane domains, the first extracellular loop, the first intracellular loop, and part of the second intracellular loop of the A_{2B}R. This fragment was subjected to a random mutagenesis PCR reaction and reintroduced in an otherwise wild type receptor, resulting in a library of approximately $4 \cdot 10^6$ plasmids containing mutant A_{2B}Rs. The library was screened for mutant receptors displaying constitutive activity and/or an increase in potency of the full A_{2B}R agonist NECA using a yeast system with growth as a simple read-out. This yeast strain has been genetically modified to enable mammalian GPCRs to couple to the yeast pheromone pathway that is subsequently able to stimulate transcription of the reporter gene HIS3. The ability of the yeast cell containing an active receptor to produce histidine can be used in a yeast growth assay on histidine-deficient medium, where growth of the yeast cells is positively correlated with activation of the adenosine A_{2B} receptors.

From the random mutagenesis screen only one receptor was identified containing mutations in the first extracellular loop. This receptor was found having two single point mutations simultaneously at positions corresponding to residues 71 (F71L) and 74 (D74G) in the protein structure (**Figure 1**). No combination of mutations at these positions with mutations in another area of the fragment was identified. Activation assays showed that the double mutant receptor showed a 2.6-fold increased level of

constitutive activity as well as a 2.7-fold increased potency for NECA compared to the wild type receptor (see also **Table 1**).

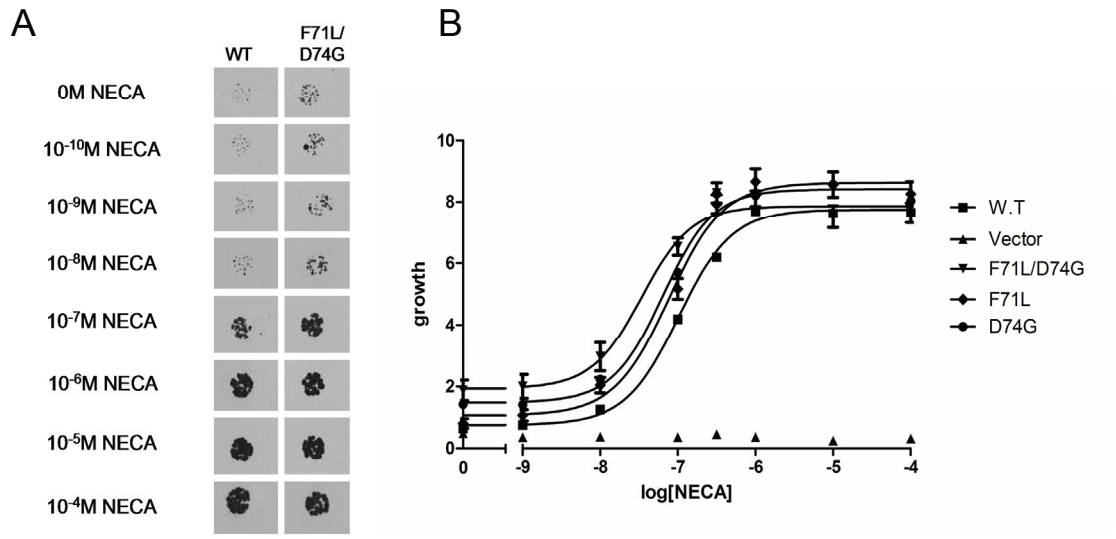

Figure 2. Receptor activation in a yeast growth assay. Yeast growth was measured with increasing NECA concentrations on selective agar plates lacking the markers uracil, leucine, and histidine. *(A)* Yeast growth density of a representative experiment, as seen on the solid selection plates. Growth of the MMY24 yeast strain expressing the wild-type (WT) human $A_{2B}R$ and of the strain expressing the double mutant receptor $A_{2B}R$_F71L/ D74G in the presence of varying concentrations of NECA. (*B*) Concentration-response curves of the WT (■) and mutant receptors F71L/D74G (▼),F71L (♦), and D74G (●).

Mutants in EL1 change potency of the agonist NECA

To decipher the role of the individual amino acids, we generated single point mutants F71L and D74G using site-directed mutagenesis. These mutants were also expressed in the MMY24 *S. cerevisiae* strain. The density of growth of the yeast cells that were transformed with the mutant receptors was monitored in response to the full agonist NECA on solid selection medium (**Figure 2**). Both single point mutants F71L and D74G show a concentration-response curve that is in between the double mutant and the wild type curves. The EC_{50} values of NECA were 67 and 47 nM on the F71L and D74G mutant receptor, respectively. Both receptors displayed constitutive activity as well, albeit less than the double mutant (see also **Tables 1 and 2**). Western blotting showed similar expression of all mutants compared to the wild type receptor (**Figure 3**).

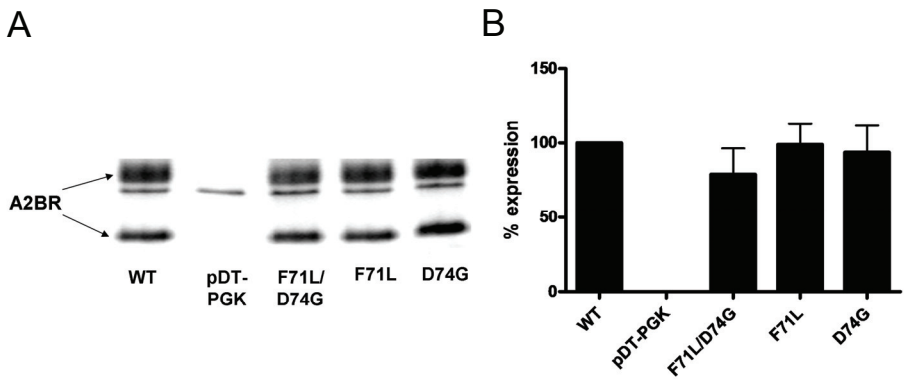

Figure 3. (*A*) Western blot showing expression levels of wild-type (WT) receptor, empty vector pDT-PGK, and mutants F71L/D74G, F71L, and D74G. Arrows indicate specific bands belonging to the adenosine A_{2B}R.
(B) Densitrometric analysis of the western blot showing relative expression levels compared to WT.

The inverse agonist ZM241385 inhibits constitutive activity of the mutant receptors

The activity of some mutant receptors was measured in response to an inverse agonist for the A_{2B}R, ZM241385. Only the mutants with more than twice the level of constitutive activity compared to the wild type, F71L/D74G and D74G, were studied. When adding 10 μM ZM241385 to the cultures, we observed that levels of constitutive activity of the mutant receptors F71L/D74G and D74G were suppressed to wild type levels (**Figure 4**). This suggests that the mutant receptors are still able to bind the inverse agonist ZM241385 and to reach an inactive state.

Figure 4. Effects of the inverse agonist ZM241385 on yeast growth. Growth was measured on selective agar plates, YNB-ULH, in the absence or presence of 10 μM of the inverse agonist ZM241385.
Vertical bars represent fold activity of the double-mutant F71L/D74G and the single-mutant D74G, compared to basal activity of the wild-type (WT) human A_{2B}R. Growth of yeast transformed with the empty vector pDT-PGK was measured as negative control.

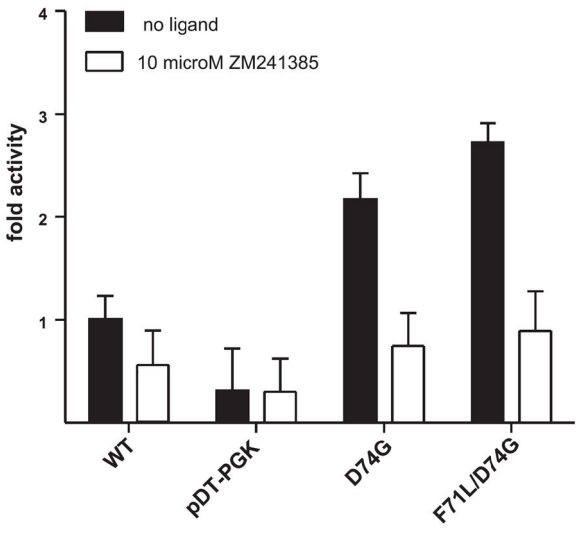

Site-saturation Mutagenesis

Next, site-saturation mutagenesis was performed on positions 71 and 74 of the $A_{2B}R$. From each of the two mutagenesis sites, 100 colonies were chosen for identification. Saturation mutagenesis at position 71 yielded 14 other amino acids. Only residues asparagine, glutamine, proline, threonine, and tryptophan, were not found. From saturation mutagenesis at site 74, 16 other naturally occurring amino acids were retrieved; residues histidine, methionine, and proline could not be identified in this case. The activity profiles of all retrieved mutants were tested in the yeast growth assay using solid selection medium as described previously.

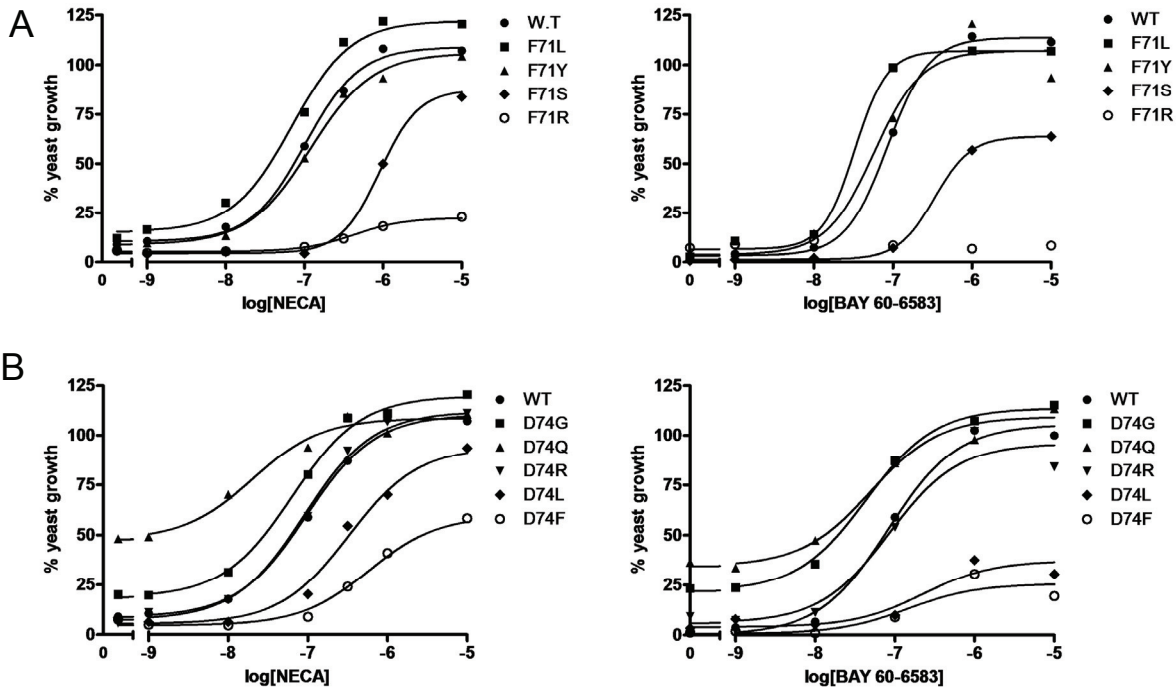

Figure 5. (A) Representative concentration-growth curves of F71X *(A)* and D74X mutant receptors *(B)*. Yeast growth was measured on selective agar plates YNB-ULH with increasing NECA or BAY 60-6583 concentrations. Mutant receptors F71L (■), F71Y (▲), F71S (♦), and F71R (○) show the variety in concentration-growth curves of the mutant receptors resulting from saturation mutagenesis. As a reference, the concentration-growth curve of the wild type human $A_{2B}R$ (●) is shown.

The mutant receptors at position 71 can be divided into two groups; mutant receptors with i) similar activation profiles compared to the wild type receptor and with ii) a decreased level of activity. In **Figure 5A**, a few representative concentration-growth curves are shown that demonstrate the range of different activation profiles. The first group comprising receptors in which the phenylalanine was mutated into an isoleucine, glutamic acid, tyrosine, lysine, and methionine, did not display a change in

activity levels (**Table 1**). Mutation into valine induced a small, but significant decrease in potency. The second group includes mutations that cause a large decrease in levels of activity or even a complete loss of activation. Residues belonging to this second group are histidine, aspartic acid, cysteine, serine, arginine, alanine, and glycine. All of these mutant receptors showed a decrease in NECA potency of at least 4-fold compared to the wild type receptor. The F71 mutant receptors that displayed the largest decrease in potency, with serine, arginine, alanine, or glycine, also showed a decrease in maximum intrinsic activity. Only the originally identified mutant F71L showed a small, but significant increase in potency. Besides the well characterized adenosine receptor agonist NECA, the activation profile of the mutant receptors was also investigated using the non-nucleoside agonist BAY 60-6583 [23]. This agonist represents a new class of adenosine receptor ligands, showing agonistic effect without having a ribose moiety. This chemically different agonist showed effects on the mutant receptor similar to the activation with NECA (**Figure 5A, Table 1**).

Activation profiles of mutations introduced at position 74 showed an even larger variation. In **Figure 5B**, several representative concentration-growth curves are depicted that demonstrate this variation in activation profiles in response to NECA as well as to BAY 60-6583. A number of mutations induced at position 74 caused an increase in potency and constitutive activity. These involve changing the aspartic acid into a glutamine, glutamic acid, asparagine or serine residue. Mutations into a lysine, tyrosine, alanine, arginine, or threonine, did not affect the response to NECA. However, when the aspartic acid was mutated into a tryptophan, cysteine, leucine, valine, phenylalanine or isoleucine, the activity was decreased or even lost. Most mutant receptors resembled the intrinsic activity of the wild type receptors or even showed a slight increase in maximal activation levels in response to NECA. However, residues cysteine, leucine, phenylalanine, and isoleucine, caused a decrease in intrinsic activity. The effects of the mutations at position 74 on receptor activity in response to the agonists NECA or BAY 60-6583 are summarized in **Table 2**. The effects of both agonists on the mutant receptors relative to the wild type receptor are similar.

Table 1. Characterization of the adenosine receptor A_{2B} receptor mutants at position 71 resulting from saturation mutagenesis. EC_{50} values (nM) are shown as means ± SEM of at least three independent experiments, each performed in duplicate. The mean values derived from the concentration-growth curves were used for calculation of the fold EC_{50} value, fold constitutive activity (CA), and percentage maximal activity (Emax), compared to the wild type receptor. The Emax represents the intrinsic activity of the receptor.

	NECA 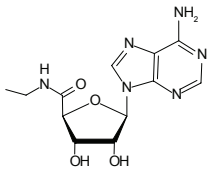			BAY 60-6583 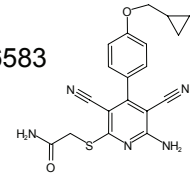		
Mutant	Fold CA	EC_{50} (nM)	Fold EC_{50}	% Emax	EC_{50} (nM)	Fold EC_{50}
WT	1.0	94±11	1.0	100	81±14	1.0
F71L/D74G	2.6	35±6	0.4	100	49±14	0.6
F71L	1.4	67±14	0.7	110	65±22	0.8
F71I	0.9	108±23	1.2	100	132±44	1.6
F71E	0.7	118±20	1.3	100	134±17	1.7
F71K	1.0	124±16	1.3	100	110±42	1.4
F71M	1.0	130±34	1.4	100	114±13	1.4
F71Y	0.9	147±36	1.6	100	101±12	1.3
F71V	0.7	167±21	1.8	100	171±29	2.1
F71H	0.3	437±58	4.6	100	226±9	2.8
F71D	0.5	442±105	4.7	95	387±123	4.8
F71C	0.2	589±74	6.2	100	312±24	3.9
F71S	0.4	933±157	9.9	82	319±19	3.9
F71R	0.5	N.D.	N.D.	21	N.D.	N.D.
F71A	0.5	N.D	N.D.	9	N.D.	N.D.
F71G	0.5	N.D	N.D.	5	N.D.	N.D.

Table 2. Characterization of the mutants at position 74 of the adenosine receptor A_{2B} receptor resulting from saturation mutagenesis. EC_{50} (nM) values are shown as means ± SEM of at least three independent experiments, each performed in duplicate. The mean values derived from the concentration-growth curves were used for calculation of the fold EC_{50} value, fold constitutive activity (CA), and percentage maximal activity (Emax), compared to the wild type receptor. The Emax represents the intrinsic activity of the receptor.

	NECA 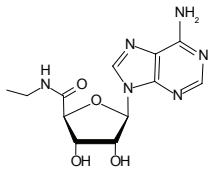			BAY 60-6583 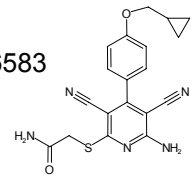		
Mutant	Fold CA	EC_{50} (nM)	Fold EC_{50}	% Emax	EC_{50} (nM)	Fold EC_{50}
WT	1.0	94±11	1.0	100	81±14	1.0
F71L/D74G	2.6	35±6	0.4	100	49±14	0.6
D74G	2.0	47±9	0.5	107	43±6	0.5
D74Q	4.8	30±6	0.3	100	35±7	0.4
D74E	2.2	49±5	0.5	109	66±11	0.8
D74N	3.5	61±14	0.7	103	45±16	0.5
D74S	4.3	68±23	0.7	104	48±7	0.6
D74K	2.2	84±11	0.9	107	85±17	1.0
D74Y	2.4	84±14	0.9	104	70±29	0.9
D74A	1.8	91±7	1.0	108	144±26	1.8
D74R	0.9	97±8	1.0	100	83±9	1.0
D74T	1.6	108±17	1.2	106	135±46	1.7
D74W	0.8	197±20	2.1	103	152±54	1.9
D74C	0.3	256±47	2.7	107	156±10	1.9
D74L	0.6	323±64	3.4	85	188±41	2.3
D74V	0.7	333±39	3.5	100	242±83	3.0

Radioligand binding to EL1 mutants

For further characterization of the EL1 mutant receptors retrieved by site-saturation mutagenesis, we performed radioligand binding experiments using the $A_{2B}R$ selective antagonist [^{3}H]PSB-603 [24]. Most mutant receptors showed specific binding of [^{3}H]PSB-603 similar to the wild type A_{2B} receptor. Only mutants F71K and D74N caused an increase in specific binding. Mutant receptor D74G showed a decreased specific binding of the radioligand compared to the wild type receptor, even though this receptor displayed an increase in potency in response to NECA and BAY 60-6583. Mutant receptors that led to a large decrease in agonist potency as observed in the solid growth assays, generally also showed decreased binding of the antagonist [^{3}H]PSB-603 (**Figure 6**).

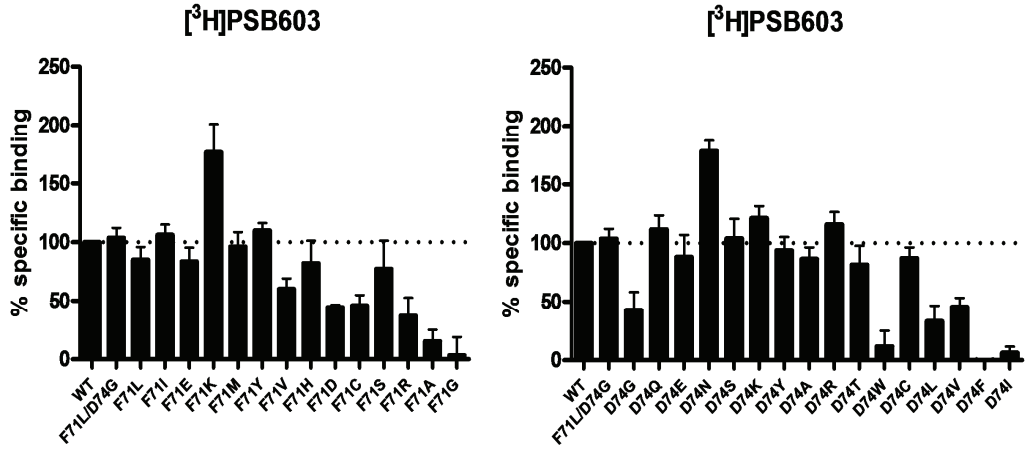

Figure 6. Single point competition binding assay with [^{3}H]PSB603. Binding experiments were performed at a radioligand concentration of 0.5-0.8 nM. Nonspecific binding was determined using 1 mM NECA. Specific [^{3}H]PSB603 binding to the wild type receptor was set to 100%. The mutant receptors are shown in descending order of activation as seen in the concentration-growth curves.

To examine whether this observation might be due to a decrease in antagonist affinity, we performed a Schild plot analysis. For this purpose, we chose one mutant receptor, D74W, which showed a decreased potency to the agonists but was still able to reach maximal activation levels in the concentration-growth curves, and compared its behavior to the wild-type receptor. Concentration-growth curves of the agonist NECA were recorded in the presence of increasing concentrations of the (unlabeled) antagonist PSB603, leading to rightward shifts. A Schild analysis of the curves yielded pA_2 values of 9.7 and 9.3 for the wild-type and mutant receptor, respectively (**Figure 7**).

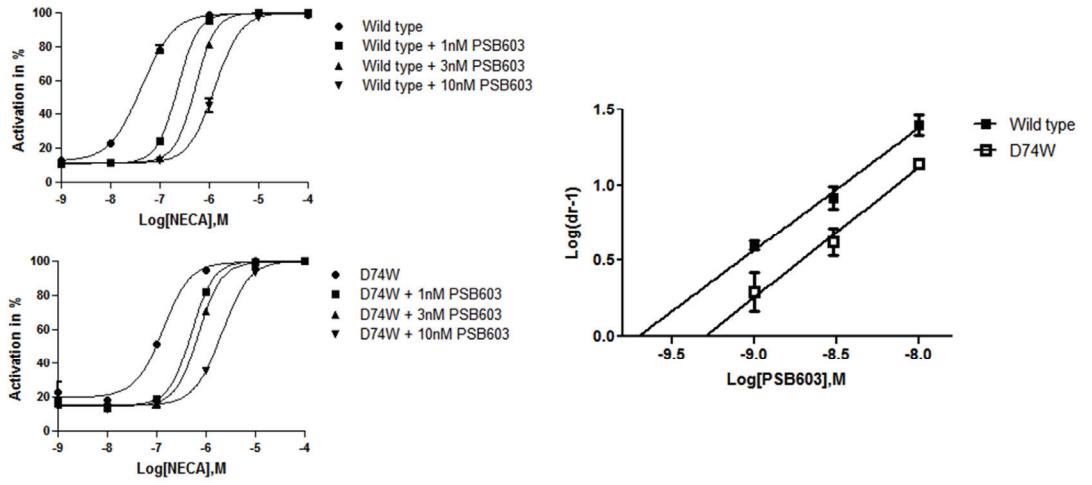

Figure 7. Schild plot analysis of PSB603 binding to WT and D74W receptors. Concentration-growth curves of NECA were recorded in the absence and presence of three concentrations of antagonist PSB603. The pA_2 value of PSB603 was determined from a Schild plot. Data are represented as mean ± SEM of three independent experiments, performed in duplicate.

DISCUSSION

A double mutant was found in a random mutagenesis study in which mutant adenosine A_{2B} receptors were selected based on their levels of increased constitutive and agonist-dependent activation. This mutant receptor contained two point mutations, both located in the first extracellular loop of the receptor. Until now, no reports have been published on this small loop as being involved in adenosine receptor activation. Both of the mutants' components, F71L and D74G, were generated through site-directed mutagenesis of the wild type A_{2B}R. Each of these two mutant receptors contributed to the effect on the receptor activity, inducing an increase in agonist potency as well constitutive activity compared to the wild type receptor. The level of constitutive activity could be inhibited to wild type levels by the inverse agonist ZM241385, showing that the mutant receptors are still functional and are not structurally locked in a certain receptor conformation.

Analysis of protein expression using Western Blotting indicated that the observed increase in receptor activation was not due to an increased expression level of the mutant receptors, which was further confirmed with radioligand binding studies (*vide infra*). Thus, the first extracellular loop appears to play an important role in the activation of the adenosine A_{2B} receptor with a special role for a phenylalanine located at position 71 and an aspartic acid at position 74.

Next, a site-saturation mutagenesis study was performed at the two positions to gain more insight in how and why this specific region is involved in the activation mechanism of the receptor. This study revealed that a single amino acid change at either of the two positions may result in a large alteration in activation profile. Quite a few of the residues at position 71 that enable the receptor to be fully activated by NECA share similar properties. They are like phenylalanine itself large, hydrophobic and bulky amino acids, such as (iso)leucine, tyrosine and methionine. However, glutamate and lysine are equally tolerated, which both are charged amino acids. Radioligand binding experiments revealed that almost all mutated receptors show similar binding of the antagonist [^{3}H]PSB603, indicating a similar expression profile. Only the mutant receptor with a lysine at the 71 position showed an increase in binding, which could be due to an increased affinity of the antagonist or a higher expression of the receptor. Several mutant receptors with a decreased potency to NECA, also showed a lower binding of [^{3}H]PSB603. This combined finding might be due to a decrease in receptor expression, but is most likely caused by a decrease in antagonist affinity, which we established to be the case for a mutation on position 74, discussed in the next paragraph. There is one other publication describing the influence of aromatic residues in EL1 on receptor activation. Härterich et al identified an aromatic π-stacking region in the neurotensin 1 receptor that might provide rigidity to the loop. Mutagenesis of these aromatic residues in EL1 interfered with receptor activation and strongly reduced ligand binding [27].

Mostly polar residues were found that maintain receptor activity at position 74. Charged residues seem to be equally favorable on this position. Both positively charged residues arginine and lysine show a potency to NECA similar to the wild type receptor, whilst glutamic acid with a negative charge like the wild-type aspartic acid, shows a two-fold increase in potency. The other residues that cause an increase in potency for NECA are glutamine and asparagine, the uncharged homologues of glutamic and aspartic acid, respectively. As was observed for the 71 position, binding of mutated receptors at the 74 position to the antagonist [^{3}H]PSB603 is mostly similar to the wild type receptor. It is therefore most likely that changes in receptor activation are not due to changes in receptor expression levels. Only mutant receptor D74N showed an increase in specific radioligand binding and might thus be expressed in higher amounts. When the aspartic acid was mutated into a glycine antagonist binding was decreased, even though its activation in response to an agonist was

increased. Its expression level in the immunoblot (**Figure 3**) was similar to that of the wild type receptor. Other mutant receptors with lower specific binding of the radioligand also showed a decreased activation profile with NECA. This could be due to a decrease in expression levels, but is more likely to be the result of a decrease in affinity to the antagonist. For this reason, a Schild plot analysis was performed using the mutant receptor D74W. This mutation caused a decrease in agonist potency, but was still able to induce maximal activation. The Schild plot indeed showed that the affinity for the antagonist PSB603 was decreased compared to the wild type receptor, which, as a consequence, may have yielded less specific binding of the radioligand at the concentration used.

Activation studies were also performed in the presence of a structurally different agonist, BAY 60-6583. This agonist lacks a ribose group that was previously thought to be important for agonist function and represents a new class of adenosine receptor agonists [23]. Concentration-growth curves of this agonist yielded similar results as seen with NECA, showing that the effects on activation are not specific for one chemical class of agonists.

Several studies on GPCRs have reported an important role for charged residues within the first extracellular loop in receptor activation, such as for the Ste2p receptor, the $VPAC_1$ receptor, and the V_{1a} vasopressin receptor. These reports confirm our finding that the polar nature of these residues promotes receptor activation [28,29,30,31].

EL1 in receptor activation

Contrary to the transmembrane domains, the extracellular loops of G protein-coupled receptors are highly divergent. Even within subfamilies, the amino acid sequence of the extracellular loops can vary greatly. This holds true for the subfamily of adenosine receptors as well. Compared to the high sequence similarity of the transmembrane domains among the adenosine receptor family (87% similarity and 71% identity between the four adenosine receptor subtypes), even the small first extracellular loop shows little resemblance. However, when investigating this sequence in the A_{2B} receptor among different species, we learned that this region is highly conserved (data not shown).

Table 3. Single point mutations reported in the first extracellular loop of other class A GPCRs. Mutations affecting receptor activation at the equivalent position of F71 and D74 in the $A_{2B}R$.

Position equivalent to F71			
Receptor	Mutation	Effect	Reference
CCKAR	F107A	Decrease in affinity as well as agonist potency	[32]
CCR5	W94A	Decreased receptor activity	[33]
CCKBR	F120A	Slightly reduced affinity for agonist	[34]
NK2R	W99C	Loss of affinity for agonist and antagonist	[35]
V2aR	F105V	Increase in agonist potency	[36]
Position equivalent to D74			
Receptor	Mutation	Effect	Reference
C5aR	G105D	Increase in affinity for agonist	[37]
RHO	G106W	Decreased levels of functional receptor in the plasma membrane	[38]

An investigation among all class A GPCRs shows that even though the amino acid sequence of the first extracellular loop can vary greatly, its length differs little. In fact, over 90% of class A GPCRs have between 50 and 53 amino acids in between the conserved 2.50 and 3.50 residues [39], which sequence stretch includes EL1. The adenosine A_{2B} receptor is among this majority. The conservation in length of the loop throughout the class A GPCR family could indicate a similar role for the first extracellular loop in receptor activation. Positions 71 and 74 in the $A_{2B}R$ are equivalent to the first and last residues of the WXFG motif described by Klco and co-workers [5]. The authors describe a role of this motif in activation, but not in ligand binding of the C5aR. However, disruption of the residues in the WXFG motif resulted in a loss of affinity for the ligand in other receptors, such as the tachykinin NK2 receptor and the AT_1 receptor [35,40]. The WXFG motif is widespread as it is present in most non-olfactory class A GPCRs. However, no such motif is present in adenosine receptors. Several mutations described in literature are listed in **Table 3**; these are located at positions equivalent to F71 and D74 in EL1. All of these mutations resulted in a change in receptor activation, showing some precedence for our findings. Further emphasis on the importance of the first extracellular loop in

GPCR activation stems from several somatic mutations, some of which have been implied to cause pathology. In patients with retinitis pigmentosa, two residues in the first extracellular loop of rhodopsin were found to be mutated [41,42]. A mutation in the vasopressin V2 receptor causes diabetes insipidus due to an increased potency for the agonist [36]. In the first extracellular loop of GPR54 a leucine was substituted by a proline, completely inhibiting signaling through the PLC pathway and causing isolated hypogonadotropic hypogonadism [43]. In the TSH receptor, two somatic mutations of a hydrophobic residue in EL1 causing constitutive activity of the receptor were found in hyperfunctioning thyroid adenomas [44].

Crystal structure of A_{2A}R as a model

Until now, the crystal structures of only a small number of class A GPCRs have been elucidated. All show a different conformation of the extracellular loops. The human adenosine A_{2A} receptor is the most recent structure published [4]. Of all G protein-coupled receptors, the A_{2B}R is most closely related to this receptor. Also, their first extracellular loops are similar. We have created a chimeric homology model of the A_{2B}R based on the A_{2A}R structure but carrying the EL1 of the A_{2B} receptor. As a result of the model building the numbering changed; F70 corresponds to F71 (A_{2B}R) and D73 to D74 (A_{2B}R) (**Figure 8**). The non-conserved disulfide bridge (C71-C159) between the centers of EL1 and EL2 that is unique in this crystal structure remains in place after a limited molecular mechanics optimization, indicating that the A_{2B}R is likely to have structural features in EL1 similar to the A_{2A}R. The most prominent motif in the extracellular region of the A_{2A}R structure is an anti-parallel β-sheet that is formed between EL1 and EL2, with the disulfide bridge in the centre connecting C71 in EL1 and C159 in EL2. The cysteines involved in this disulfide bond are only conserved in subtype 2 of the adenosine receptors (A_{2A}R and A_{2B}R). Together with the disulfide bridge between EL2 and the top of TM3 that is conserved among most class A GPCRs, this second cysteine bridge provides extra stability and causes EL2 to bend more closely to EL1. Even though the second extracellular loop differs greatly between the A_{2A}R and the A_{2B}R in length and in sequence, the cysteine involved in the nonconserved disulfide bond between EL1 and EL2 can be very well aligned in the two receptors. From this sequence alignment, it is plausible that in the A_{2B}R, this disulfide bond is present between C72 in EL1 and C167 in EL2. Many

GPCRs also contain additional, not conserved, extracellular cysteine residues that can form disulfide bonds that influence the tertiary receptor structure and receptor stability [45,46,47].

Several lipophilic residues are present within a radius of approximately 5 Å of the phenylalanine at position 71 in the crystal structure of the $A_{2A}R$ as well as in our chimeric $A_{2B}R$-$A_{2A}R$ model. All of these residues are pointing towards the protein. The phenylalanine is buried in between these lipohilic side chains and forms the onset of the anti-parallel β-sheet. At position 74, the aspartic acid is involved in receptor activity and is pointing outward in the aqueous environment. This spatial orientation, in which the phenylalanine is directed towards the protein and the aspartic acid is pointing outwards, is consistent with the presence of a β-sheet in which residues alternate above and below the sheet [48]. It is likely that the β-sheet's stability is altered (and hence the receptor activity), when (the properties of) positions 71 and 74 are changed.

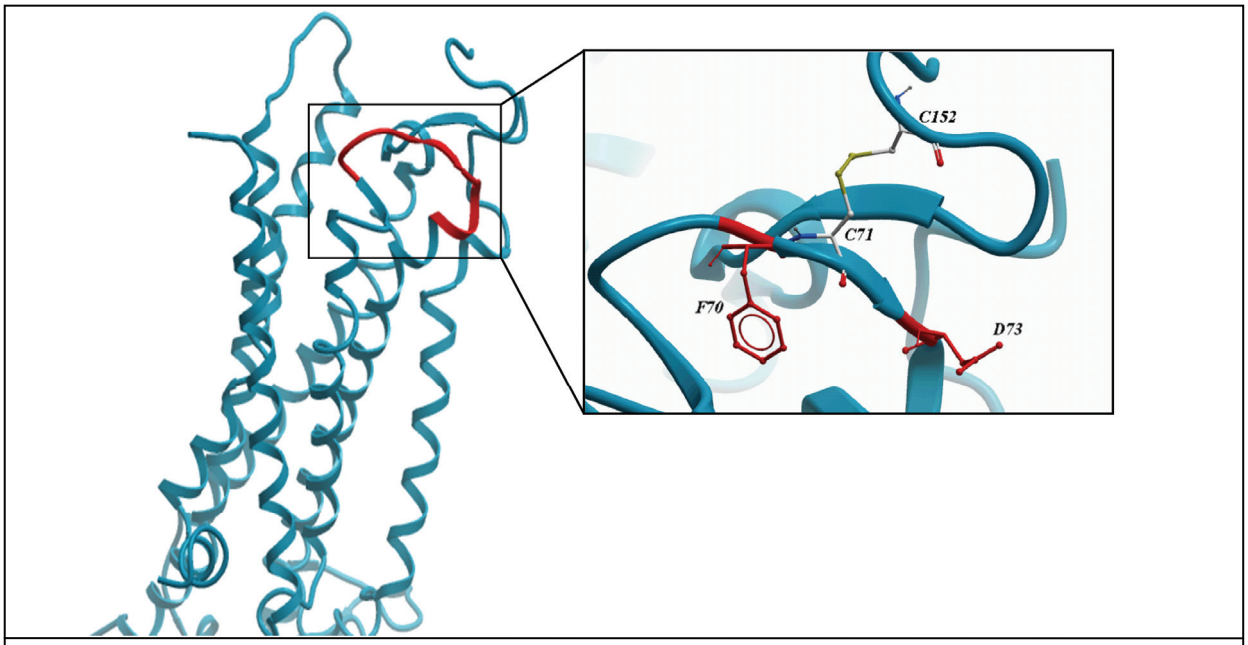

Figure 8. Ribbon representation of the chimeric receptor model based on the adenosine A_{2A} receptor structure (PDB: 3EML), carrying the EL1 of the $A_{2B}R$. The $A_{2A}R$ structure is shown in cyan, the $A_{2B}R$ EL1 in red. Inset: detailed view of the extracellular region, including the EL1. Here, the whole structure is colored cyan. The locations of the mutations are displayed in red; positions 70 and 73 correspond to the residues F71 and D74 in the $A_{2B}R$. The antiparallel β-sheet between EL1 and EL2 is shown by two arrows in the ribbon structure. The side chains of the cysteines forming the nonconserved disulfide bridge (C71-C159) are also shown with the sulfur atoms in yellow.

In conclusion, we have identified two residues located in the first extracellular loop, a phenylalanine and an aspartic acid, which are involved in the activation of the adenosine A_{2B} receptor. Site-saturation mutagenesis and activation growth studies in yeast have shown that a polar residue is necessary at position 74. At position 71, an amino acid appears to be required that can be buried in the vicinity of neighboring lipophilic residues pointing towards the transmembrane regions. Assuming that the first extracellular loop of the A_{2B}R adopts a similar tertiary structure as has been observed for the A_{2A}R, residues F71 and D74 are located at the verge of an anti-parallel β-sheet formed by EL1 together with EL2. Our results indicate that this unique structural feature is essential for normal receptor activation and mutations that alter the β-sheet's stability result in a large impact on the receptor's constitutive and agonist-induced activity. Given the conserved length of the first extracellular loop as well as other mutagenesis reports implicating this loop as being involved in activation, a similar function for the EL1 as described in this report might be the case in other class A GPCRs. However, since the presence of an anti-parallel β-sheet has so far only been established in the adenosine receptor structure, the activating influence of EL1 in other receptors may proceed through different structural features.

ACKNOWLEDGEMENTS

This research was performed under the auspices of the GPCR Forum, a program funded by the Dutch Top Institute Pharma (project D1-105).

REFERENCES

[1] Olah, M.E., Jacobson, K.A., Stiles, G.L., *J Biol Chem* (1994) 269:24692-24698.
[2] Klco, J., Wiegand, C., Narzinski, K., Baranski, T., *Nat Struct Mol Biol.* (2005) 12:320-326.
[3] Massotte, D., Kieffer, B.L., *Nat Struct Mol Biol* (2005) 12:287-288.
[4] Jaakola, V.P., Griffith, M.T., Hanson, M.A., Cherezov, V., Chien, E.Y., Lane, J.R., IJzerman, A.P., Stevens, R.C., *Science* (2008) 322:1211-1217.
[5] Klco, J., Nikiforovich, G., Baranski, T., *J Biol Chem.* (2006) 281:12010-12019.
[6] Vassart, G., Pardo, L., Costagliola, S., *Trends Biochem Sci* (2004) 29:119-126.
[7] Nurwakagari, P., Breit, A., Hess, C., Salman-Livny, H., Ben-Menahem, D., Gudermann, T., *J Mol Endocrinol* (2007) 38:259-275.
[8] Kleinau, G., Jaeschke, H., Mueller, S., Raaka, B.M., Neumann, S., Paschke, R., Krause, G., *Faseb J* (2008) 22:2798-2808.

[9] Sura-Trueba, S., Aumas, C., Carre, A., Durif, S., Leger, J., Polak, M., de Roux, N., *Endocrinology* (2009) 150:1043-1050.
[10] Mizutori, Y., Chen, C.R., McLachlan, S.M., Rapoport, B., *Mol Endocrinol* (2008) 22:1171-1182.
[11] Fredholm, B.B., Arslan, G., Halldner, L., Kull, B., Schulte, G., Wasserman, W., *Naunyn Schmiedebergs Arch Pharmacol* (2000) 362:364-374.
[12] Fredholm, B.B., IJzerman, A.P., Jacobson, K.A., Klotz, K.N., Linden, J., *Pharmacol Rev* (2001) 53:527-552.
[13] Wilson, C.N., *Br J Pharmacol* (2008) 155:475-486.
[14] Spicuzza, L., Di Maria, G., Polosa, R., *Eur J Pharmacol* (2006) 533:77-88.
[15] Hasko, G., Linden, J., Cronstein, B., Pacher, P., *Nat Rev Drug Discov* (2008) 7:759-770.
[16] Brown, A., et al., *Yeast* (2000) 16:11-22.
[17] Stewart, G.D., Valant, C., Dowell, S.J., Mijaljica, D., Devenish, R.J., Scammells, P.J., Sexton, P.M., Christopoulos, A., *J Pharmacol Exp Ther* (2009) 331:277-286.
[18] Beukers, M., van Oppenraaij, J., van der Hoorn, P., Blad, C., den Dulk, H., Brouwer, J., IJzerman, A., *Mol Pharmacol.* (2004) 65:702-710.
[19] Beukers, M., IJzerman, A., *Trends Pharmacol Sci.* (2005) 26:533-539.
[20] Fromant, M., Blanquet, S., Plateau, P., *Anal Biochem* (1995) 224:347-353.
[21] Olesnicky, N.S., Brown, A.J., Dowell, S.J., Casselton, L.A., *Embo J* (1999) 18:2756-2763.
[22] Li, Q., Ye, K., Blad, C.C., den Dulk, H., Brouwer, J., IJzerman, A.P., Beukers, M.W., *J Pharmacol Exp Ther* (2007) 320:637-645.
[23] Eckle, T., et al., *Circulation* (2007) 115:1581-1590.
[24] Borrmann, T., Hinz, S., Bertarelli, D.C., Li, W., Florin, N.C., Scheiff, A.B., Muller, C.E., *J Med Chem* (2009) 52:3994-4006.
[25] Chemical Computing Group, I., Molecular Operating Environment, Quebec, Canada, 2008.
[26] Wang, J., Cieplak, P., Kollman, P., *J Comput Chem* (2000) 21:1049-1074.
[27] Härterich, S., Koschatzky, S., Einsiedel, J., Gmeiner, P., *Bioorg Med Chem* (2008) 16:9359-9368.
[28] Bajaj, A., Connelly, S.M., Gehret, A.U., Naider, F., Dumont, M.E., *Biochim Biophys Acta* (2007) 1773:707-717.
[29] Langer, I., Vertongen, P., Perret, J., Waelbroeck, M., Robberecht, P., *Neuropharmacology* (2003) 44:125-131.
[30] Hauser, M., Kauffman, S., Lee, B.K., Naider, F., Becker, J.M., *J Biol Chem* (2007). 282(14):10387-97.
[31] Hawtin, S., Simms, J., Conner, M., Lawson, Z., Parslow, R., Trim, J., Sheppard, A., Wheatley, M., *J Biol Chem.* (2006) 281:38478-38488.
[32] Archer-Lahlou, E., Tikhonova, I., Escrieut, C., Dufresne, M., Seva, C., Pradayrol, L., Moroder, L., Maigret, B., Fourmy, D., *J Med Chem* (2005) 48:180-191.
[33] Genoud, S., Kajumo, F., Guo, Y., Thompson, D., Dragic, T., *J Virol* (1999) 73:1645-1648.
[34] Langer, I., Tikhonova, I.G., Travers, M.A., Archer-Lahlou, E., Escrieut, C., Maigret, B., Fourmy, D., *J Biol Chem* (2005) 280:22198-22204.
[35] Labrou, N.E., Bhogal, N., Hurrell, C.R., Findlay, J.B., *J Biol Chem* (2001) 276:37944-37949.
[36] Pasel, K., Schulz, A., Timmermann, K., Linnemann, K., Hoeltzenbein, M., Jaaskelainen, J., Gruters, A., Filler, G., Schoneberg, T., *J Clin Endocrinol Metab* (2000) 85:1703-1710.
[37] Cain, S.A., Woodruff, T.M., Taylor, S.M., Fairlie, D.P., Sanderson, S.D., Monk, P.N., *Biochem Pharmacol* (2001) 61:1571-1579.
[38] Sung, C.H., Schneider, B.G., Agarwal, N., Papermaster, D.S., Nathans, J., *Proc Natl Acad Sci U S A* (1991) 88:8840-8844.
[39] Ballesteros, J.A., Weinstein, H., *Methods Neurosci* (1995) 25:366–428.
[40] Hjorth, S.A., Schambye, H.T., Greenlee, W.J., Schwartz, T.W., *J Biol Chem* (1994) 269:30953-30959.
[41] Fishman, G.A., Stone, E.M., Gilbert, L.D., Sheffield, V.C., *Arch Ophthalmol* (1992) 110:646-653.
[42] Vaithinathan, R., Berson, E.L., Dryja, T.P., *Genomics* (1994) 21:461-463.
[43] Tenenbaum-Rakover, Y., Commenges-Ducos, M., Iovane, A., Aumas, C., Admoni, O., de Roux, N., *J Clin Endocrinol Metab* (2007) 92:1137-1144.
[44] Parma, J., Van Sande, J., Swillens, S., Tonacchera, M., Dumont, J., Vassart, G., *Mol Endocrinol* (1995) 9:725-733.
[45] Noda, K., Saad, Y., Graham, R.M., Karnik, S.S., *J Biol Chem* (1994) 269:6743-6752.
[46] Dohlman, H.G., Caron, M.G., DeBlasi, A., Frielle, T., Lefkowitz, R.J., *Biochemistry* (1990) 29:2335-2342.
[47] Moro, S., Hoffmann, C., Jacobson, K., *Biochemistry* (1999) 38:3498-3507.

[48] Branden, C., Tooze, J., Introduction to protein structure, Garland Publishing, New York and London, 1991.